

Forecasting the effect of COVID-19 on the S&P500

Karina Arias-Calluari* and Fernando Alonso-Marroquin†
School of Civil Engineering, The University of Sydney, Australia

Morteza. N. Najafi
Department of Physics, University of Mohaghegh Ardabili, Ardabil, Iran

Michael Harré
Complex Systems Research Group, Faculty of Engineering, The University of Sydney, Australia

The outbreak of the novel coronavirus (COVID-19) has caused unprecedented disruptions to financial and economic markets around the globe, leading to one of the fastest U.S. stock market declines in history. However, in the past we have seen the market recover and we can expect the market to recover again, and on this basis we assume the Standard and Poor's 500 (S&P500) index will reach a minimum before rising again in the not-too-distant future. Here we present four forecast models of the S&P500 based on COVID-19 projections of deaths released on 02/04/2020 by the University of Washington and the 2-months consideration since the first confirmed case occurred in USA. The decline and recovery in the index is estimated for the following three months. The forecast is a projection of a prediction with fluctuations described by q -gaussian distributions. Our forecast was made on the premise that: (a) The prediction is based on a deterministic trend that follows the data available since the initial outbreak of COVID-19, and (b) fluctuations derived from the S&P500 over the last 24 years.

I. INTRODUCTION

Immediately following the outbreak of COVID-19, epidemiological researchers from around the world have produced an extensive array of analyses in order to model the spread, growth, peak, and ultimately the decline of the disease [1–5]. For countries like China, Japan, Italy, and Iran, their epidemiological curve of COVID-19 progression displays a peak before the second month since the first cases were detected [6–8]. In countries like the UK, Australia and Germany, the governments have taken mitigation measures to slow the impact [1, 2]. As a consequence, these countries display a flattening of the caseload curves with a peak generally estimated to be somewhere between the second to fourth month since the first diagnosed cases.

The simultaneous reaction of governments, companies, consumers and media, have created a demand and supply shock, making COVID-19 a qualitatively different economic crisis than previous crises [9]. This economic ‘wedging’ of falling supply and demand is caused by rapidly escalating unemployment decreasing consumer demand where, in the US for example, 17 million Americans have applied for unemployment insurance in the first three weeks of the crisis [10], and businesses are closing their doors reducing the supply of manufactured goods across the globe [11]. As a consequence financial markets around the world have fallen precipitously and market volatility is at near-all-time highs [12]. For example the S&P500 has registered the worst one-day fall in the last

24 years and the third biggest percentage loss in its history.

Events such as COVID-19 pose systemic *exogenous* risks to markets, similar to the September 11 2001 attacks or the 1995 Kobe earthquake [13] in that the events cannot be endogenised into market prices by ‘rational’ agents ahead of time because they are not foreseeable. Alternatively *endogenous* systemic risks are an inherent part of the nonlinear dynamics of a market and may have detectable precursor signals that act as warnings similar to those used in other nonlinear systems such as climate and ecology [14]. As an example the 1987 market crash is likely an endogenous event [13] and it has been shown that it had a measurably different effect on market dynamics from that of the September 11 attacks [15]. Endogenous risks can be modelled in a microeconomic fashion by considering the interactions between agents and how these change over time, causing non-linear disruptions even if system parameters change in a smooth fashion [16, 17]. The effects of these changes are likely causes of abrupt changes at the macro level of market dynamics [18, 19]. In both cases the market response can be decomposed into two parts, a response function that models changes in the overall trend of the system, called the skeleton [20], and the other is the stochastic term. In this work we are interested in the nonlinear properties of both of these terms.

In the uncertain environment of COVID-19 it is difficult to forecast the fluctuations of the S&P500. We then need assumptions such as the mortality rates due to COVID-19 or the duration of the current shutdown of economic activity. Our central assumption is based on a predicted peak for COVID-19 deaths. Current results in Figure 1 based on the daily World Health Organization reports [21] show that the S&P500 responds to the

* karina.ariascalluari@uni.sydney.edu.au

† fernando.alonso@sydney.edu.au

inflection points of the cumulative amount of deaths and confirmed cases with no lag. This fact supports our assumption that when a peak number of deaths occurs, the market reaches a stationary point.

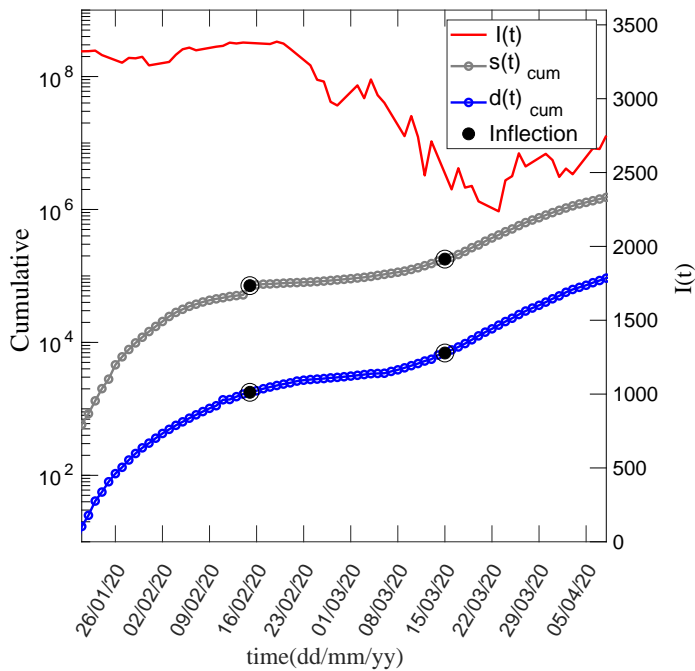


Figure 1. The S&P500 decreased after the WHO (World Health Organization) reported an increment in confirmed cases $s(t)$ and number of deaths $d(t)$ due to COVID-19. The increments in the number of cases are represented with a black filled point, which are an abrupt change of slope of the first derivative of $s(t)_{cum}$ and $d(t)_{cum}$.

We developed two cases, in the first case the peak number was located on the 23rd of May by the University of Washington [22]. The second case is where the peak number of deaths is considered 2-months since the first death occurred [23]. After this point we expect a recovery period as economic activity starts to return to normal. To construct the forecast, we assume that the stock market index can be decomposed into a deterministic trend and a stationary stochastic fluctuation. The statistics of the fluctuation have been obtained by analyzing the S&P500 index during the 24 year period from January 1996 to March 2020 [24]. $I(t_0)$ is the initial point of the stock market index for some time point t_0 , and the index $I(t)$ for $t > t_0$ is its time evolution. In these predictions we take $t_0 = 24/03/2020$ and $t_0 = 28/02/2020$ for the two different forecast. The price return at time t is defined by:

$$X(t) = I(t_0 + t) - I(t_0). \quad (1)$$

In earlier work we used a detrended fluctuation approach

[24] to decompose the price return $X(t)$ into a deterministic component $\bar{X}(t)$ and a stationary *fluctuating component* $x(t)$

$$X(t) = \bar{X}(t) + x(t). \quad (2)$$

The trend $\bar{X}(t)$ was obtained by averaging the index over a moving time window. The size of the window was one year, that was optimized to guarantee that the fluctuations around the trend exhibit stationary behavior. By using a curve-fitting analysis on the S&P500 data over the past 24 years (see Appendix), we show that the probability density function (PDF) of the detrended price is well described by the functional form:

$$p(x, t) = \frac{1}{(Dt)^{1/\alpha}} g_q \left(\frac{x}{(Dt)^{1/\alpha}} \right), \quad (3)$$

where D , q and α are time-dependent fitting exponents. The g_q term is the q -Gaussian function defined as:

$$g_q(x) = \frac{1}{C_q} e_q(-x^2) \quad (4)$$

and the q -exponential function is $e_q(x) = [1 + (1 - q)x]^{1/(1-q)}$ that reduces to the exponential function when $q \rightarrow 1$. The normalization constant C_q for $1 < q < 3$ is given by:

$$C_q = \sqrt{\frac{\pi}{q-1} \frac{\Gamma((3-q)/(2(q-1)))}{\Gamma(1/(q-1))}}. \quad (5)$$

The cumulative distribution function (CDF) of the PDF (Eq.3) of the detrended price return is;

$$F(x, t) = \int_{-\infty}^x p(x, t) dx. \quad (6)$$

The complementary of the CDF is used here to quantify risk under extreme events [25]. This is defined as probability that $X - \bar{X}$ lies outside the interval $[-x, x]$ is

$$P(X(t) - \bar{X}(t) > |x|) = 1 - \int_{-x}^x p(x, t) dx. \quad (7)$$

For this paper we introduce the standarization of the q -error function

$$\text{erf}_q(x) = 2 \int_0^x g_q(y) dy \quad (8)$$

The standard error function is a special case of the q -error function for $q = 1$. Considering this definition, Eq.7 is written as:

$$P(X(t) - \bar{X}(t) > |x|) = 1 - \text{erf}_q(x/(Dt)^{1/\alpha}). \quad (9)$$

We use Eq. (9) to develop a forecast of the market based on the historical fluctuations in the S&P500. Figure 2 shows some key dates over the last 24 years of the S&P500. The market dynamics consists of periods of

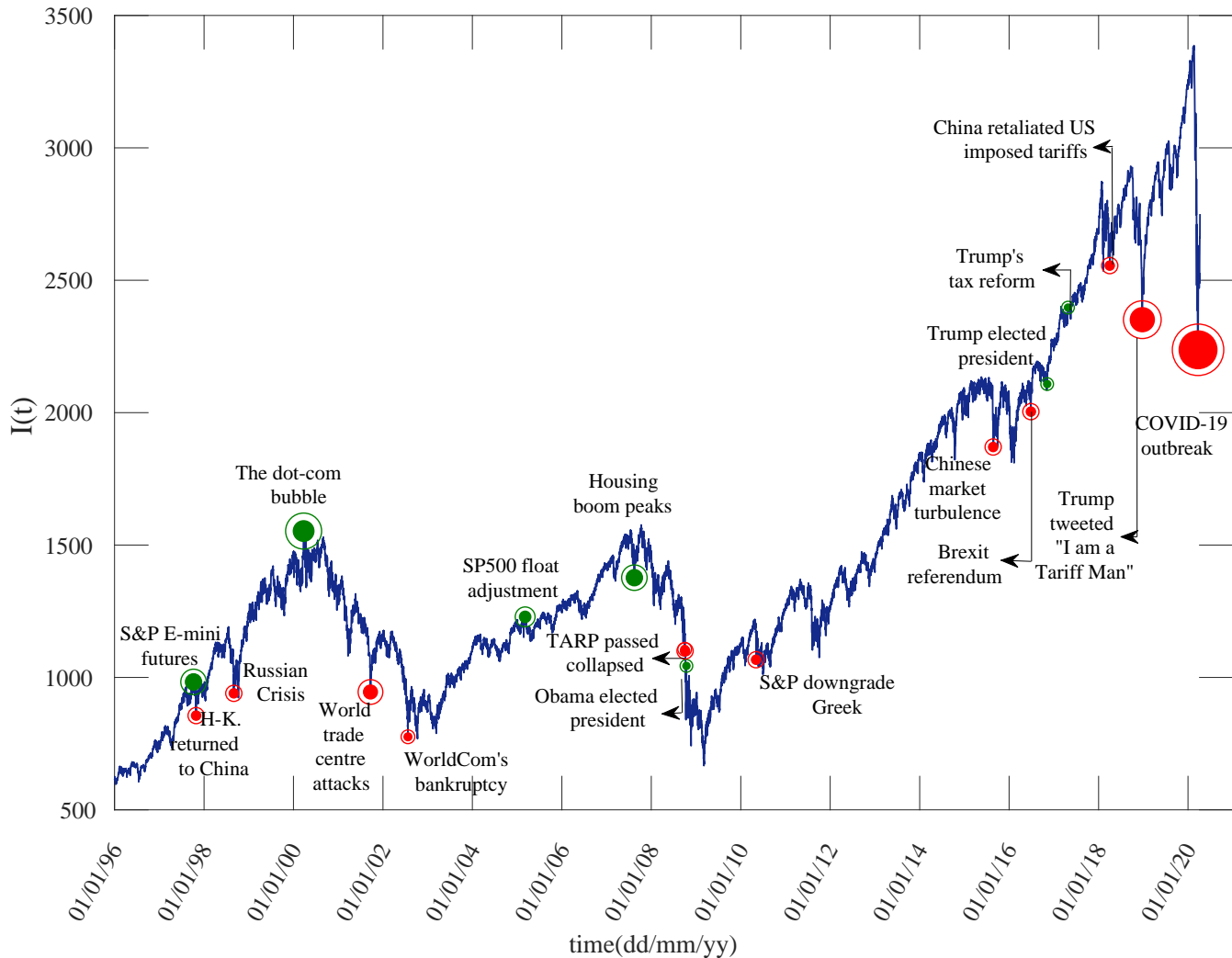


Figure 2. The S&P500 index $I(t)$ from 02/01/96 to 24/03/20 (24 years). In this data set the largest daily percentage loss of -11.98% was registered on 16/03/20. Some other key events are also shown for reference.

a bull market (systematic increase of the index) and a bear market (systematic decrease). The crashes in this plot are discontinuous. They occur in a very short period of time that we attribute as noise that it is added to the deterministic component. For example, during the Global Financial Crisis (GFC) there is a long-term decline in the value of the S&P500 that we can interpret as the deterministic trend, but near the point where Lehman Brothers collapses there is a discontinuous market crash. In fact, there are several very large daily price movements that are not always attributable to a specific event. These ‘crashes’ (both up and down) are more similar to large stochastic movements, not a part of the deterministic component of the market dynamics.

To establish the effect of COVID-19 on the market we assume that it has a deterministic, exogenous impact. This impact is assumed to be a response function that

corresponds to a COVID-19 induced bear market followed by a smooth transition to a bull market. As a further refinement we assume that this transition is dictated by a key quantitative factor: the estimated date on which the mortality rate peaks. Our first estimation of this trend (private communication, April 2, 2020 [26]) was based on the time-frame from 31/01/2020 to 24/03/2020 in which a bear-market decline in $I(t)$ had already been observed. For the construction of the deterministic trend $\tilde{I}(t)$ the parabola and hyperbola functions were used. For the parabola three conditions were applied and are illustrated in Figure 3: (i) The initial point of the predicted trend at t_0 is $\tilde{I}(t_0)$, (ii) the slope of $\tilde{I}(t)$ at t_0 is obtained from a linear fitting during the interval 31/01/2020 to 24/03/2020, (iii) the point where the recovery is pre-

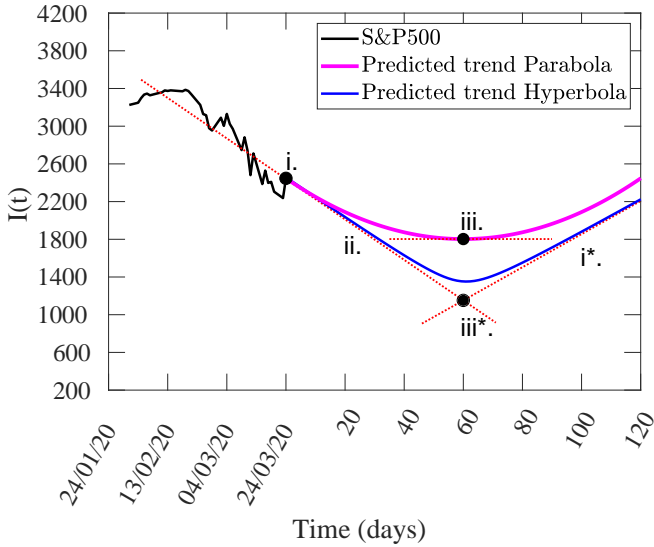


Figure 3. A downward trend followed by a market recovery i estimated by applying a parabolic fitting (magenta line) an hyperbola fitting (blue line). Three steps were applying t define each deterministic trend. The step ii is the same for both cases.

dicted at 60 days satisfies $\tilde{I}'(t_0 + 60 \text{ days}) = 0$, i.e.

$$\left. \frac{\tilde{I}(t)}{dt} \right|_{t_0+60 \text{ days}} = 0. \quad (10)$$

For the hyperbola three similar conditions were applied: The slope of the market recovery (bull market) (i^*) is assumed to be 0.5 of the slope of the market's collapse similar to the previous crashes that have occurred over the past 24-years. The slope (ii) is the same as the parabola and point (iii^*) is the intersection of the slopes (i^*) and (ii). For both methods the point (iii) was based on the public information available by the University of Washington where the death rate was estimated to peak on 24/05/2020 (60 days from t_0). To obtain this prediction of the trend we assumed that there is no time lag between the peak of mortality rate and the time where the market starts to recover.

Up to this point we have evaluated the systemic risk as the deterministic aspect of the market evolution, which is often neglected by analysts in the determination of the impact of exogenous events such as the COVID-19 pandemic. In what follows we evaluate the risk associated with the stochastic fluctuations of the index by 'dressing' the deterministic risk with a q -Gaussian diffusion process. In a previous publication [27] we found that the q -Gaussian fluctuations of the S&P500 index around the trend have distinctive super-diffusion spatio-temporal regimes ('space' refers to the size of the fluctuations). To allow long-term forecasting on the order of days, we have extended the analysis for longer times. Three well-defined regimes are observed in Fig. 4,

- Zone A: Strong superdiffusion process with short-time correlations
- Zone B: Weak superdiffusion process with weak time correlations
- Zone C: Normal diffusion process with no time correlations.

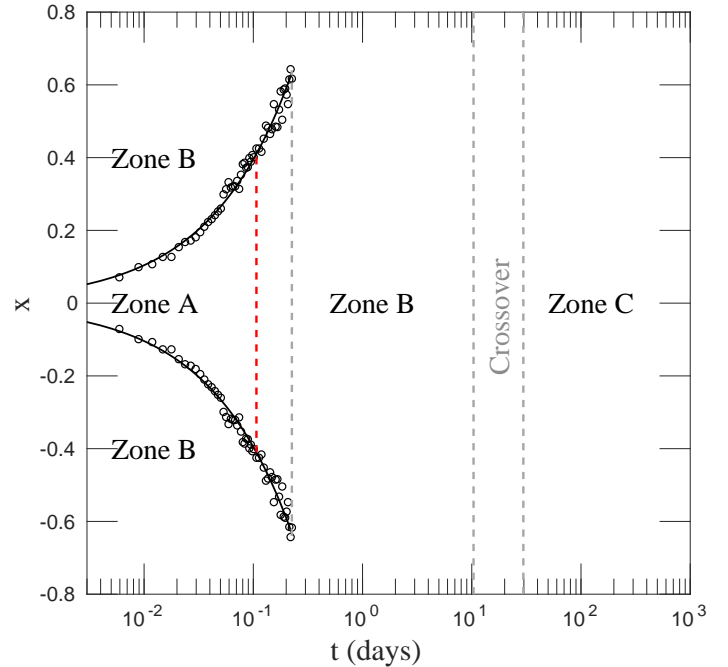


Figure 4. Three different zones were determined based on an abrupt slope change of α and q values. The circles represent the end points of the strong super-diffusion regime (zone A) from t_0 to $t = 35$ minutes. The remaining area during the first 35 minutes to 28 days corresponds to a weak super-diffusion regime (zone B). A normal diffusion process is reached after thirty days. The gray dashed lines represent the transitions between each zone.

These zones are well-distinguished in time, where Zone A goes from 0 to 38 minutes, Zone B from 10 days to 28 days and after a crossover period Zone C starts at 30 days (Fig. 4). Note that the time series tends to a classical diffusion process for large times, in agreement with the classical Central Limit Theorem. See [27] for a complete analysis of these zones and their derivation.

Two techniques were used to calculate the optimal q for each $p(x, t)$, one focusing on the PDF and the other focusing on each CDF. For the first technique two methods were used. The least square method and q -moments method. The least square method applies Eq.3 as the fitting function. The q -moments method uses a system of two equations and two variables, q and α . The first equation is given by the "second moment" or variance $\langle x^2 \rangle$. The second equation refers to the "escort second moment" or q -variance $\langle x^2 \rangle_{q_2}$. In general, the q -moments are applied to PDFs with asymptotic decays because they

provide finite values [28]. The second technique is based on each CDF, where a least squares method is applied using Eq.A7. The quality of the fitting models were evaluated based on the smoothness of the time evolution of the CDF. The best results were obtained with the second technique. We extend the analysis of this derivation in the supplementary materials section.

The corresponding q , α and D values that fit each of these equations are displayed in Fig.A.1(a-c-d). The q and β values were calculated directly after fitting Eq.A7. The α values are calculated as the power law of the β value, by averaging the power law over a moving time window smaller than the transition zone. The D value is calculated by replacing α in Eq.A5. The results for q , α and D obtained by applying the least squares method of the CDFs are consistent with the ones calculated focused on the PDFs. The convergence of $q \rightarrow 1$ and $\alpha \rightarrow 2$ shows that the PDF of x is Gaussian when $t \rightarrow \infty$.

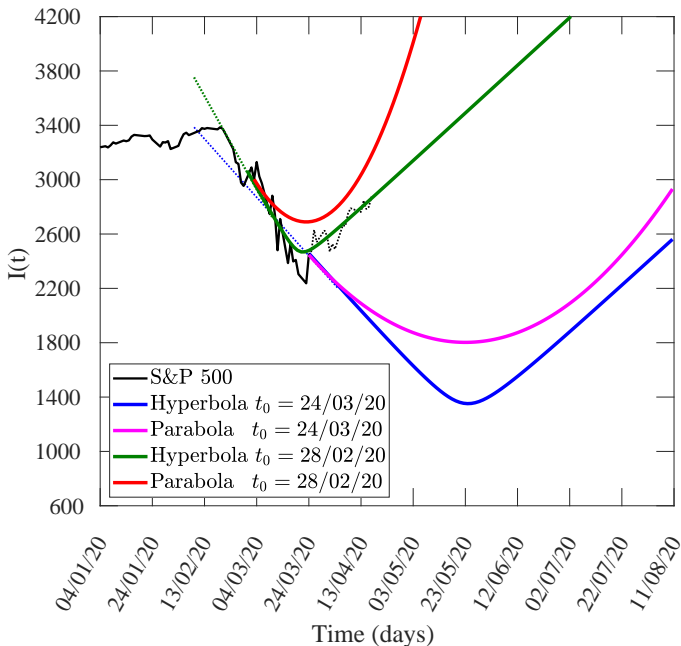


Figure 5. The decline and recovery on four different trends due to COVID-19 are observed. The first forecast method considers $t_0 = 24/03/2020$ and the second one $t_0 = 28/02/2020$. For both cases a parabola and hyperbola fitting was used, considering the method previously illustrated in Fig. 3. The hyperbola method with $t_0 = 28/02/2020$ displays the most accurate result at the moment.

We then construct a forecast of the S&P500 using two predicted trends, the parabola and the hyperbola shown in Fig.5. We note that these trends are approximations based upon the prices for the following trading days. For that reason both trends were re-calculated using $t_0 = 28/02/2020$; the date on which the first death occurred in USA; and $I'(60) = 0$; two months after the first case was confirmed. These new trends display a bet-

ter performance, notably the hyperbola which fits better than the others.

The the uncertainty was modeled with the analytical form of the detrended price by replacing the $\alpha(t)$, $q(t)$, and $D(t)$ calculated in the Appendix into Eq.3 with their numerical estimates. Once the stochastic term is simulated it is added into the deterministic trend to see the full stochastic path of $I(t)$.

Figure 6 shows the forecast result identifying the range of possibilities during the market's decline and subsequent recovery. The predicted trend was plotted as a hyperbola with $t_0 = 28/02/2020$ (Figure 5). The uncertainty is presented by a shaded contour plot with a scale from 0 to 1. These values represent the probability of a possible variation of $P(X - \bar{X} > |x|)$ which can be visualized as a "cone of uncertainty". This probabilistic path of the S&P500 over the following 60 days (2 months) shows the evolution of the PDF of $I(t)$, which diffuses as t increases. Also we see that the real data for index after t_0 (the dashed line) lies within a tiny interval in the vicinity of the predicted trend, mainly in the most probable (dark) regions, verifying that our model is working and is reliable for forecasting with 85% of accuracy.

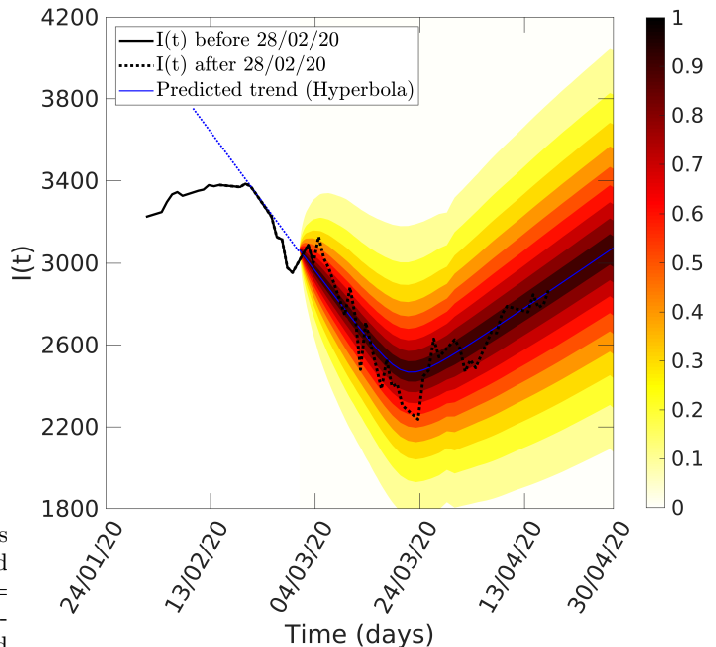


Figure 6. The decline and recovery on $I(t)$ due to COVID-19 is observed from 28/02/20 to the following 2 months. A downward and upward market predicted trend is calculated by applying a hyperbolic fitting with no time lag. The uncertainty is represented by a scale from 0 to 1, where represent the $P(X - \bar{X} > |x|)$ of each contour line. The economy will start its recovery after this epidemic peak of deaths

We construct a forecasting based on essential public information provided by the University of Washington on their web page[21]. A good forecasting is always an

iterative process that can be daily updated considering new factors and changes.

In summary, we have presented a model of the stochastic and systematic risk in the stock market and applied it to forecast the stock market response to COVID-19. We have assumed that the stochastic risk is a q -Gaussian diffusion process. The systemic risk is the deterministic aspect of the market evolution that is often neglected by market analysts but here we have assumed that COVID-19 has a deterministic, exogenous impact on the market. We have dressed this nonlinear skeleton with a q -Gaussian diffusion process that we developed in previous work. The response function we have used for forecasting is a simple behavioural model based on the assumption that markets recover once prices drop to sufficiently low

enough levels, in future work it can be improved by developing better tools to evaluate systematic risk using behavioural [29] or macroeconomic [30] models. In addition, our stochastic method is still heuristic and it needs to be developed by formulating the governing equations that allows transition from strong- to weak- superdiffusion and converging to a normal diffusion process for large times, as dictated by the classical Central Limit Theorem.

We acknowledge Australian Research Council grant DP170102927. K.A.C. thanks The Sydney Informatics Hub at The University of Sydney for providing access to HPC-Artemis for financial data processing. We thanks Sornette, Tsallis and Christian Beck for inspiring discussions.

-
- [1] R. M. Anderson, H. Heesterbeek, D. Klinkenberg and T. D. Hollingsworth, *The Lancet*, 2020, **395**, 931–934.
- [2] S. L. Chang, N. Harding, C. Zachreson, O. M. Cliff and M. Prokopenko, *arXiv preprint arXiv:2003.10218*, 2020.
- [3] R. A. Neher, R. Dyrdak, V. Druelle, E. B. Hodcroft and J. Albert, *Swiss Medical Weekly*, 2020, **150**, year.
- [4] C. Li, L. J. Chen, X. Chen, M. Zhang, C. P. Pang and H. Chen, *Eurosurveillance*, 2020, **25**, year.
- [5] S. Luding, *A simple qualitative multi-scale corona model (a report)*, 2020.
- [6] V. Surveillances, *China CDC Weekly*, 2020, **2**, 113–122.
- [7] D. Fanelli and F. Piazza, *Chaos, Solitons & Fractals*, 2020, **134**, 109761.
- [8] M. Abdi, *Infection Control & Hospital Epidemiology*, 2020, 1–5.
- [9] N. Fernandes, *Economic effects of coronavirus outbreak (COVID-19) on the world economy*, 2020.
- [10] S. Chaney and D. Harrison, *U.S. Jobless Claims Soar for Third Straight Week*, 2020, <https://www.wsj.com/articles/u-s-surge-in-unemployment-claims-expected-to-continue-11586424605>.
- [11] S. Donnan, C. Rauwald, J. Deaux and I. King, *A Covid-19 Supply Chain Shock Born in China Is Going Global*, 2020, <https://www.bloomberg.com/news/articles/2020-03-20/a-covid-19-supply-chain-shock-born-in-china-is-going-global>.
- [12] W. Watts, *Coronavirus stock-market volatility is creating the largest daily price swings since 1929 crash*, 2020, <https://www.marketwatch.com/story/stock-market-investors-have-to-go-back-to-1929-to-find-daily-swings-this-wild-2020-04-07>.
- [13] D. Sornette, in *Extreme events in nature and society*, Springer, 2006, pp. 95–119.
- [14] T. M. Lenton, *Nature Climate Change*, 2011, **1**, 201–209.
- [15] M. Harré and T. Bossomaier, *EPL (Europhysics Letters)*, 2009, **87**, 18009.
- [16] D. H. Wolpert, M. Harré, E. Olbrich, N. Bertschinger and J. Jost, *Physical Review E*, 2012, **85**, 036102.
- [17] M. S. Harré and T. Bossomaier, *Entropy*, 2014, **16**, 5102–5121.
- [18] J.-P. Onnela, A. Chakraborti, K. Kaski and J. Kertesz, *Physica A: Statistical Mechanics and its Applications*, 2003, **324**, 247–252.
- [19] M. Harré, Proceedings of the International Conference on Social Modeling and Simulation, plus Econophysics Colloquium 2014, 2015, pp. 15–25.
- [20] C. H. Hommes, *Financial markets as nonlinear adaptive evolutionary systems*, Taylor & Francis, 2001.
- [21] W. H. Organization, *Coronavirus disease (COVID-2019) situation reports*, 2020, <https://www.who.int/emergencies/diseases/novel-coronavirus-2019/situation-reports>.
- [22] T. I. for Health Metrics and E. (IHME), *COVID-19 Projections*, 2020, <http://www.healthdata.org/covid/data-downloads>.
- [23] C.-C. Lai, T.-P. Shih, W.-C. Ko, H.-J. Tang and P.-R. Hsueh, *International journal of antimicrobial agents*, 2020, 105924.
- [24] K. Arias-Calluari, M. Najafi, M. S. Harré, F. Alonso-Marroquin *et al.*, *arXiv preprint arXiv:1910.01034*, 2019.
- [25] M. Haas and C. Pigorsch, *Encyclopedia of Complexity and Systems Science*, 2009, **4**, 3404–3435.
- [26] K. Arias-Calluari and F. Alonso-Marroquin, Private Communication, 2020.
- [27] F. Alonso-Marroquin, K. Arias-Calluari, M. Harré, M. N. Najafi and H. J. Herrmann, *Physical Review E*, 2019, **99**, 062313.
- [28] C. Tsallis, A. R. Plastino and R. F. Alvarez-Estrada, *Journal of Mathematical Physics*, 2009, **50**, 043303.
- [29] S. Bikhchandani and S. Sharma, *IMF Staff papers*, 2000, **47**, 279–310.
- [30] M. Gertler, N. Kiyotaki and A. Prestipino, in *Handbook of Macroeconomics*, Elsevier, 2016, vol. 2, pp. 1345–1425.

Appendix A: Supplementary materials

The probability density function (PDF) of the detrended price is well described by the functional form:

$$p(x, t) = \sqrt{\beta} g_q \left(\sqrt{\beta} x \right), \quad (\text{A1})$$

where, $\beta = (Dt)^{-2/\alpha}$, allows to recovery Eq. 3.

Then, a system of two equations based on variance $\langle x^2 \rangle$ and q -variance $\langle x^2 \rangle_{q_2}$ were used to obtain the q and β values.

The variance $\langle x^2 \rangle$ has a finite value for $q < 5/3$;

$$\langle x^2 \rangle = \frac{1}{\beta(5-3q)}. \quad (\text{A2})$$

The normalized q -variance $\langle x^2 \rangle_q$ is defined as [28]

$$\langle x^2 \rangle_q = \frac{\int_{-\infty}^{\infty} x^2 p(x, t)^q dx}{\int_{-\infty}^{\infty} p(x, t)^q dx}, \quad (\text{A3})$$

In general, the q -moments are calculated on PDFs with heavy tails because they provide finite values. The q -moments and the standard moments are equal for $q = 1$.

To obtain the analytical solution of the integral in the numerator and denominator of Eq. A3, we notice that

$$K(\beta, q) \equiv \int_{-\infty}^{\infty} [1 - (1-q)\beta x^2]^{\frac{1}{1-q}} dx = \frac{C_q}{\sqrt{\beta}},$$

and also the second moment of x is proportional to $\partial\beta K(\beta, q)$, so the analytical solution of the numerator is:

$$\begin{aligned} \frac{\partial}{\partial\beta} K(\beta, q) &= - \int_{-\infty}^{\infty} x^2 [1 - (1-q)\beta x^2]^{\frac{q}{1-q}} dx \\ &= - \frac{1}{2} \beta^{-3/2} C_q \end{aligned}$$

Then, the analytical solution of the denominator is:

$$\int_{-\infty}^{\infty} p(x, t)^q dx = \frac{3-q}{2}$$

Inserting this identity into the Eq. A3, we obtain:

$$\langle x^2 \rangle_{q_2} = \frac{1}{(3-q)\beta}. \quad (\text{A4})$$

The equation system is defined by Eqs.A2 and A4 and is used to calculate β and q as a function of time. The α and D values are calculated using:

$$\beta = (Dt)^{-2/\alpha} \quad (\text{A5})$$

We divide the data of S&P500 in overlapping time windows not longer than the transition zones. In each window the exponent of the power law relation is calculated and then the Eq.A5 is used to calculate D and α . The results for q, α and β are shown in Subfigures a-1,b-1,c-1 and d-1.

In Subfigure a-1 an abrupt transition in q is noticed when $t = 30$ days. This abrupt change leads to a discontinuity in the fitted function $q(t)$.

We have used an alternative method to extract the parameters, for which this discontinuity is absent. This method is based on the fitting of the $F(x, t)$ of real price return x . The analytical expression of $F(x, t)$ is obtained in terms of the $\text{erf}_q(x, t)$. First, Eq.6 is replaced in Eq. 7,

$$P(X(t) - \bar{X}(t) > |x|) = 2 - 2F(x, t). \quad (\text{A6})$$

Then, Eq. A6 and Eq.9 are compared, resulting to ($s = x\sqrt{\beta}$):

$$F(x, t) = 0.5 + \frac{\text{erf}_q(s)}{2} \quad (\text{A7})$$

Where,

$$\text{erf}_q(s) = \frac{2\sqrt{\beta}}{C_q} x {}_2F_1 \left[\frac{1}{2}, \frac{1}{q-1}, \frac{3}{2}, (1-q)s^2 \right]. \quad (\text{A8})$$

The Eq. A7 is used to calculate q and β value as a function of time. The α values are calculated again with Eq. A5 by overlapping time windows, and then, D is obtained by replacing α in A5.

These results are shown in the second column of Figure A.1. The Subfigure (a-2) does not display an abrupt transition of q value. For β, α and D the transitions are smooth in each zone.

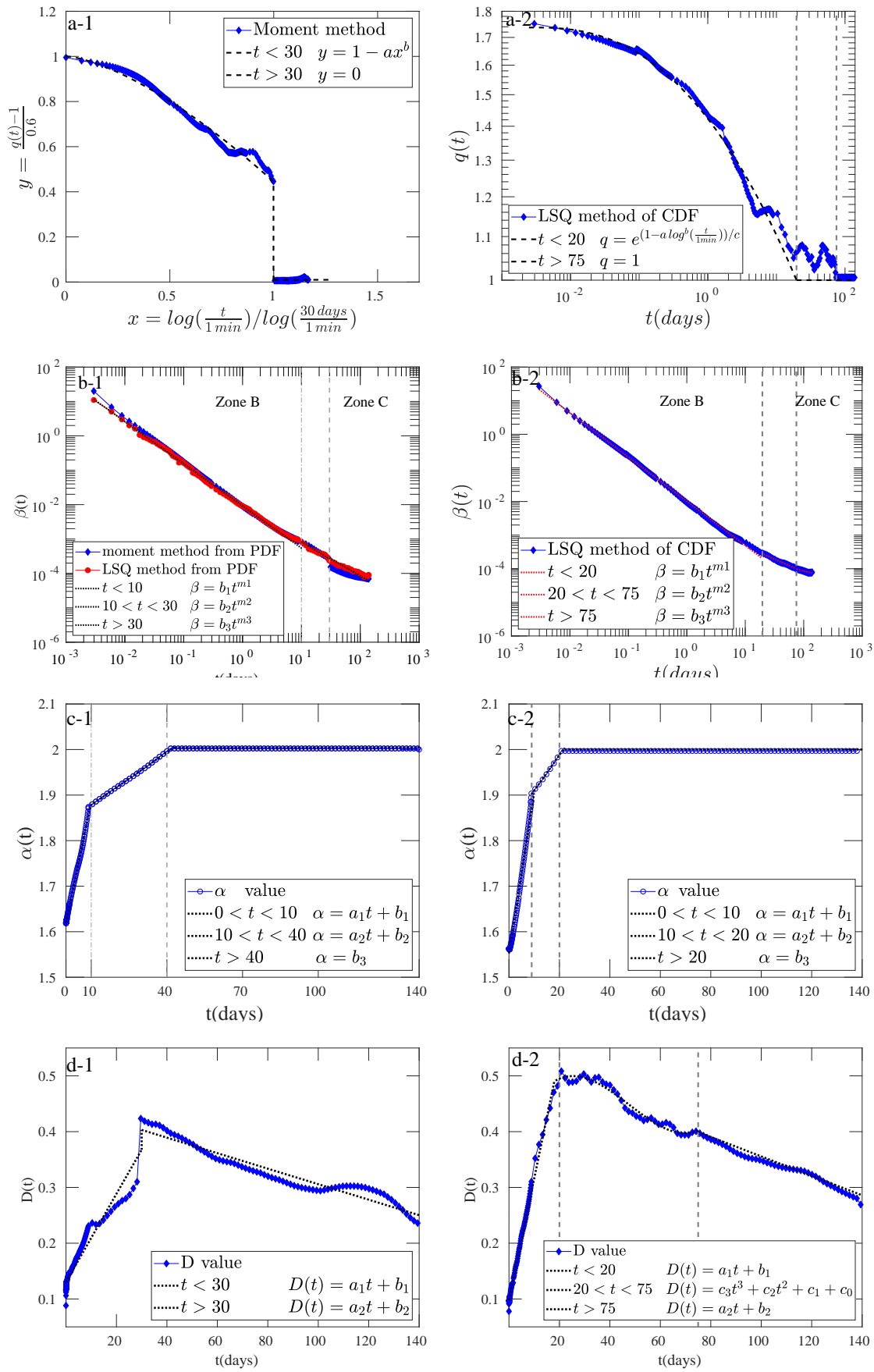


Figure A.1. Calculation of q and β by applying a Equation system [Eqs.A2 and A4] and fittings of $F(x, t)$. (a-1, a-2) Estimation of $q(t)$ value, for (a-1) a normalization of units was made. (b-1,b-2) The value of $\beta \sim t^{-2/\alpha}$. (c-1,c-2) The exponent of the power law relation of β vs t per time window is calculated as $\alpha(t)$. (d-1,d-2) The D value is calculated by replacing α in Eq.A5. The convergence to a Normal distribution function is observed when $t \rightarrow \infty$ with $q = 1$ and $\alpha = 2$. (coefficients are in Table I)

Table I. Coefficients values of fittings

	Fitting $p(x, t)$	Fitting $F(x, t)$
q	$a = 0.556 \pm 0.012$ $b = 1.485 \pm 0.041$	$a = 0.005 \pm 0.001$ $b = 2.473 \pm 0.158$ $c = 1.811 \pm 0.031$
β	$b_1 = 0.009 \pm 3.09(10)^{-4}$ $m_1 = -1.23 \pm 0.01$ $b_2 = 0.008 \pm 3.5(10)^{-5}$ $m_2 = -1.10 \pm 0.01$ $b_3 = 0.010 \pm 2.66(10)^{-4}$ $m_3 = -1.06 \pm 0.02$	$b_1 = 0.010 \pm 3.5(10)^{-5}$ $m_1 = -1.32 \pm 0.01$ $b_2 = 0.003 \pm 7.5(10)^{-4}$ $m_2 = -1.23 \pm 0.05$ $b_3 = 0.007 \pm 8.77(10)^{-4}$ $m_3 = -0.97 \pm 0.01$
α	$a_1 = 0.027 \pm 0.001$ $b_1 = 1.620 \pm 0.003$ $a_2 = 0.004 \pm 0.002$ $b_2 = 1.839 \pm 0.009$ $b_3 = 2.00 \pm 0.000$	$a_1 = 0.035 \pm 0.001$ $b_1 = 1.553 \pm 0.002$ $a_2 = 0.008 \pm 0.001$ $b_2 = 1.831 \pm 0.007$ $b_3 = 2.00 \pm 0.000$
D	$a_1 = 0.008 \pm 0.015$ $b_1 = 0.130 \pm 0.002$ $a_2 = -0.001 \pm 7.14(10)^{-5}$ $b_2 = 0.445 \pm 0.004$	$a_1 = 0.022 \pm 0.010$ $b_1 = 0.098 \pm 0.001$ $c_3 = 2.308(10)^{-6} \pm 0.765(10)^{-7}$ $c_2 = -3.30(10)^{-4} \pm 1.00(10)^{-5}$ $c_1 = 0.012 \pm 0.005$ $c_0 = 0.363 \pm 0.072$ $a_2 = -0.002 \pm 6.85(10)^{-5}$ $b_2 = 0.525 \pm 0.007$